Arg tyrosine kinase is involved in homologous recombinational DNA repair

著者	Li Yingzhu, Shimizu Hiroko, Xiang Shuang-Lin, Maru Yoshiro, Takao Noriaki, Yamamoto Ken-ichi
journal or publication title	Biochemical and biophysical research communications
volume	299
number	5
page range	697-702
year	2002-12-01
URL	http://hdl.handle.net/2297/1650

Arg tyrosine kinase is involved in homologous recombinational DNA repair

Yingzhu Li, Hiroko Shimizu, Shuang-Lin Xiang, #Yoshiro Maru, Noriaki Takao, and Ken-ichi Yamamoto§

Department of Molecular Pathology, Cancer Research Institute, Kanazawa University, Kanazawa, Ishikawa 920-0934, and the #Department of Pharmacology, Tokyo Women's Medical University, 8-1 Kawada-cho, Shinjuku-ku,, Tokyo 162-8666, Japan.

§To whom requests for reprints should be addressed, at Department of Molecular Pathology, Cancer Research Institute, Kanazawa University, 13-1 Takaramachi, Kanazawa, Ishikawa 920-0934, Japan. Phone, 81-76-265-2755; Fax, 81-76-234-4516; E-mail, kyamamot@kenroku.kanazawa-u.ac.jp;

The Abbreviations used are: A-T, ataxia telangiectasia; ATM, ataxia telangiectasia mutated; DSB, double stranded break; HR, homologous recombination; IR, ionizing radiation; PI, phosphatidylinositol

Abstract

c-Abl plays important roles in cellular response to DNA damage. However, possible roles for Arg (Abl-related gene) in DNA damage response are unknown. Here we show that ionizing radiation (IR)-induced Rad51 focus formation is reduced in *Arg*-deficient cells generated from a chicken B cell line by targeted disruption. This is consistent with the findings that *Arg*-deficient cells display hypersensitivity to IR, elevated frequencies of IR-induced chromosomal aberrations, and reduced targeted integration frequencies. All of these abnormalities in DNA damage repair are also observed in *ATM*-deficient cells but not in *c-Abl*-deficient cells. Finally, we show that Arg interacts with and phosphorylates Rad51 in 293T cells. These results suggest that Arg plays a role in homologous recombinational (HR) DNA repair by phosphorylating Rad51.

Key Words:, c-Abl family, tyrosine phosphorylation, double strand break, homologous recombinational DNA repair, Rad51 focus

Introduction

Ataxia telangiectasia (A-T) is an autosomal recessive disease characterised by radiosensitivity and chromosomal instability. The 350 kDa product of *ATM*, the gene responsible for A-T, is related to a family of large phosphatidylinositol 3 (PI3)-kinase domain-containing proteins involved in cell cycle control and/ or DNA repair. The other members of this family include ATR and DNA-dependent protein kinase. Recent work has shown ATM to act on a number of important effector proteins involved in the cellular reaction to DNA damage, including c-Abl(1). c-Abl is an ubiquitously expressed nonreceptor-type tyrosine kinase(2) and is activated by DNA damage in an ATM-dependent manner(3, 4). It plays important roles in growth arrest(5, 6) and apoptosis(7-10), and may also function in DNA repair through the phosphorylation of Rad51(11, 12), a key molecule in homologous recombinational (HR) DNA repair(13, 14).

Arg (Abl-related gene), the only other known member of the c-Abl family, shares considerable structural and sequence homology with c-Abl in the N-terminal SH3, SH2, and tyrosine kinase domains(15), and abnormal variants of Arg are implicated in some human lymphoid malignancies(16, 17). However, the roles played by Arg in the cellular response to DNA damage are unknown. In the present study, we show that *Arg*-deficient cells generated from the chicken B cell line by targeted disruption display various abnormalities in HR DNA repair. We further show that Arg associates with and phosphorylates Rad51 in vivo. Our study thus provides evidence for an Arg-Rad51 link in DNA repair.

Materials and Methods

Expression plasmids. The full-length human Arg cDNA was constructed from partial and overlapping cDNA clones, which were isolated by library screening and RT-PCR based on the published human cDNA sequences(15). The full-length Arg, c-Abl(5), and Rad51(18) cDNA expression vectors with Flag- or HA-tags (Flag-Arg-wt, Flag-c-Abl-wt, and HA-Rad51) were prepared by inserting the entire Arg, c-Abl, or Rad51 coding sequences in the correct orientation into Flag- or HA-tagged eukaryotic expression vectors driven by a human elongation factor-1 promoter (the tag sequences were located upstream of the coding sequences). The conserved lysine residues in the Arg (amino acid 337) and c-Abl (amino acid 290) tyrosine kinase domains were mutated to arginine using a PCR strategy. These kinase-dead c-Abl and Arg mutant cDNAs were then inserted into the expression vector (Flag-Arg-kd and Flag-c-Abl-kd).

Gene targeting. A partial chicken Arg cDNA was obtained by degenerative RT-PCR methods from mRNA extracted from DT40 cells. Using this cDNA fragment as a probe, chicken *Arg* genomic clones were isolated by screening an EMBL3 SP6/T7 library of genomic DNA from the liver of adult male Leghorn chicken (Clontech, Palo Alto, CA) by standard procedures. As shown in Figure 1A, about 1000 bp of the genomic sequence encoding the N-terminal portion of the chicken Arg kinase domain was replaced with selection marker gene cassettes under the control of the b-actin promoter. To generate the $Arg^{-/-}$ mutant clones, cells were transfected with a targeting vector that carried the neomycin gene, and selected in medium containing 2 mg/ml neomycin (Sigma) after the first transfection. The cells were then transfected with a histidinol-resistance cassette, and selected with both 1 mg/ml histidinol (Sigma) and 0.5 mg/ml neomycin after the second transfection. RT-PCR analysis of chicken Arg mRNA expression was performed using the following primers: 5'-AATCTGGTGCAGTTATTAGGTGTGTGTACC-3' and 5'-

AATGCCTGGGTATGGTGACATCCCATAGGT-3'.

Immunoprecipitation and immunoblotting. 293T cells were grown in Dulbecco's Modified Eagle's Medium (DMEM, Gibco-BRL, Life Technologies) supplemented with 10% heat-inactivated fetal calf serum (FCS, Gibco-BRL), 50 units/ml penicillin G, and 50 mg/ml streptomycin sulfate (Gibco-BRL) in a 5% CO_2 humidified incubator. The cells were transiently transfected with 0.5 mg of the various expression vectors as indicated in the Figures, using the calcium precipitation method. At 48 hours after transfection, whole-cell lysates were prepared and were immunoprecipitated with mouse anti-Flag (M5, Sigma) or rat high-affinity anti-HA (Roche) antibodies. Mouse anti-Flag, rat anti-HA, or mouse monoclonal anti-phosphotyrosine (4G10, Upstate) antibodies were used as the primary antibodies for immunoblotting; horse anti-mouse IgG HRP-linked (New England Biolabs) or goat anti-rat IgG HRP-linked (Funakoshi) antibodies were used as the secondary antibodies.

Immunofluorescent visualization of Rad51 foci. Rad51 foci were visualized using confocal microscopy (LSM510, Carl Zeiss Co., Ltd.) of cells stained with an anti-Rad51 antibody, as described previously(19, 20). Following microscopy and image processing with Adobe Photoshop v5.0, color-inverted images were printed and distinct Rad51 foci were counted.

Colony survival assay, karyotype analysis, and measurements of targeted integration frequencies. The measurement of surviving colonies and chromosomal aberrations following X-ray irradiation were carried out as described previously(21). Targeting with various constructs as shown in Table 2 and the subsequent analysis of drug-resistant clones were done as described previously(21). Targeting vectors for the chicken *Atr* and *JSAP2* loci will be described elsewhere.

Results and Discussion

To study possible roles for Arg in the cellular response to IR, we generated *Arg*$^{-/-}$ cells from a chicken B cell line (DT40) by targeted disruption. The *Arg* locus was disrupted by sequential transfection of the cells with two targeting vectors (Figure 1A; see Methods). The successful targeted integration was confirmed by Southern blot analysis as the appearance of mutant 8-kbp and 9-kbp KpnI genomic fragments (Figure 1B), and the disruption of the *Arg* gene was verified by RT-PCR analysis (Figure 1C).

Previous studies showed that c-Abl interacts with and phosphorylates Rad51 on tyrosine in response to DNA damage. However, the biological significance of these findings in HR DNA repair is not yet clear, as c-Abl-mediated phosphorylation negatively affected Rad51's activity in one set of experiments, but enhanced its association with Rad52 in another(11, 12). More recently, the BCR/ABL oncogenic tyrosine kinase has been shown both to enhance Rad51 expression and to phosphorylate it, resulting in drug resistance(22). On the other hand, we have recently shown that Rad51 focus formation and DSB repair capacity in *c-Abl*$^{-/-}$ DT40 cells is not grossly impaired(19), although various DSB repair defects have been well documented in *ATM*$^{-/-}$ DT40 cells(19-21). These results indicate that, while ATM are indispensable in DSB repair in eukaryotic cells, there must be redundant functions for c-Abl in DSB repair, at least in chicken DT40 cells and mouse fibroblasts(23). One possibility is that Arg substitutes for c-Abl in the genome maintenance of the *c-Abl*$^{-/-}$ cells. To clarify this issue, we analyzed the appearance of Rad51 foci in *Arg*$^{-/-}$, *c-Abl*$^{-/-}$, and *ATM*$^{-/-}$ DT40 cells following IR. Rad51 foci are subnuclear aggregates, believed to represent intermediate structures formed during the recombination required to repair radiation-induced or replication-associated DNA damage(24). As shown in

Figure 2, the disruption of *Arg* as well as of *ATM* led to impairment in the formation of Rad51 foci, although Rad51 focus formation was normal in *c-Abl*$^{-/-}$ DT40 cells.

To analyze further the DSB DNA repair capacity of *Arg*$^{-/-}$ DT40 cells, wild-type and mutant clones that were plated on methylcellulose were irradiated with 4 or 8 Gy of X-ray, and the percentage of surviving clones was determined relative to the numbers of colonies arising on untreated plates. As shown in Table 1, *ATM*$^{-/-}$ DT40 cells were extremely X-ray sensitive, as we reported previously(19-21), and *Arg*$^{-/-}$ DT40 cells were moderately sensitive; *c-Abl*$^{-/-}$ DT40 cells did not exhibit hypersensitivity to X-rays, in agreement with our recent results(19). To confirm the results of this X-ray sensitivity assay, we examined chromosomal aberrations in *Arg*$^{-/-}$ DT40 cells following IR treatment. As we reasoned and reported previously, an increase in induced chromosomal aberrations observed within 3 hours after IR (i.e., cells irradiated during the S-G_2 phase of the cell cycle) would reflect a defect in the HR repair pathway, and *ATM*$^{-/-}$ DT40 cells displayed highly increased levels of chromosomal aberrations within 3 hours of X-ray irradiation(19-21). Interestingly, disruption of *Arg* but not *c-Abl* resulted in a significant increase in chromosomal aberration frequencies (Figure 3). We further observed a slight but significant reduction in targeted integration frequencies in *Arg*$^{-/-}$ DT40 cells (Table 2), as we reported previously for *ATM*$^{-/-}$ DT40 cells(21). Consistent with these defects in DNA repair, enhanced IR-induced apoptosis was observed in *Arg*$^{-/-}$ DT40 cells (data not shown), as in *ATM*$^{-/-}$ DT40 cells(19). However, unlike in *ATM*$^{-/-}$ DT40 cells(21), IR-induced mitotic delay was normal in *Arg*$^{-/-}$ DT40 cells (data not shown). G_1/M checkpoint control has also been shown to be normal in embryonic fibroblasts derived from *Arg*$^{-/-}$/*c-Abl*$^{-/-}$ mice(25). These results thus preclude the possible involvement of cell-cycle checkpoint control abnormalities in the defective DNA repair

and apoptotic response observed in *Arg*$^{-/-}$ DT40 cells.

The above results indicate that *Arg*$^{-/-}$ DT40 cells have some HR DNA repair defects, as observed in *ATM*$^{-/-}$ DT40 cells. Furthermore, c-Abl has been shown previously to interact with and phosphorylate Rad51(11, 12). It is therefore plausible that, like c-Abl, Arg is involved in HR DNA repair through the phosphorylation of Rad51. To study this possibility, and because we had some difficulties in detecting tyrosine-phosphorylated Rad51 in DT40 cells, we transiently expressed Flag-tagged wild-type or kinase-dead Arg as well as c-Abl with HA-tagged Rad51 in 293T cells. As shown in Figure 4, the results of co-immunoprecipitation experiments showed that immunoprecipitation of wild-type but not kinase-dead Arg with an anti-Flag antibody brought down Rad51 (first row, lanes 1 and 2), indicating that Arg can interact with Rad51 in vivo. Consistent with these results, only wild-type Arg tyrosine-phosphorylated Rad51 in vivo (second row, lanes 1 and 2), indicating that the kinase activity of Arg is required for the observed tyrosine-phosphorylation of Rad51. The ineffective interaction between kinase-dead Arg and Rad51 suggests an interesting possibility that the interaction between Rad51 and Arg is further enhanced by the tyrosine-phosphorylation of Rad51 by Arg. However, we cannot rule out a possibility that this is due to a conformational change induced by the substitution of the conserved lysine residue. As reported previously(11, 12), wild-type c-Abl phosphorylated Rad51 in vivo, albeit less effectively than Arg (second row, lane 3). However, we were unable to detect the in vivo association of c-Abl with Rad51 under the conditions used in the present experiments (first row, lane 3). These results therefore indicate that Arg interacts with and phosphorylates Rad51 more effectively than does c-Abl. There have been some discrepancies about what tyrosine residues in Rad51 are phosphorylated by c-Abl; although Tyr-54 was identified in one

previous study(11), others provided evidence for Tyr-315(12, 22). In the present system, however, Arg effectively phosphorylated Rad51 with mutations at either Tyr-54 or Tyr-315 in 293T cells (unpublished data). We are working at present to identify the Arg-dependent tyrosine-phosphorylation sites in Rad51.

It has been reported previously that Arg is detected mainly in the cytoplasm(26). However, the results presented in this study indicate that disruption of *Arg* results in defective HR DNA repair functions, including reduced IR-induced Rad51 focus formation. We also showed that Arg associates with and phosphorylates Rad51. These results suggest that Arg functions in HR DNA repair through the tyrosine-phosphorylation of Rad51 in the nucleus. It is therefore possible that a small fraction of Arg might be localized and function in the nucleus, as suggested above, or that Arg might move from the cytoplasm to the nucleus, transducing signals in response to DNA damage, as c-Abl(27).

Since both of $Arg^{-/-}$ and $ATM^{-/-}$ DT40 cells display abnormalities in HR DNA repair, as shown in the present study, and since c-Abl is activated by DNA damage in an ATM-dependent manner(3, 4), it is very possible that Arg is activated by DNA damage in an ATM-dependent manner. The results of preliminary experiments in various DT40 gene-knockout cells using an antibody to human c-Abl which cross-reacts with chicken c-Abl and Arg showed that Arg is activated by IR in an ATM-dependent manner (unpublished data). However, we have been unable so far to detect the direct phosphorylation of Arg by ATM (unpublished data). The dependency of Arg activation on ATM may therefore be more complex. Further study is required to clarify this issue.

Acknowledgments

We thank Y. Shiloh for discussion and for performing the ATM phosphorylation experiments, S. Takeda for discussion, K. Yoshioka for the JSAP2 targeting vector, and A. Shinohara for human Rad51 cDNA and the antibody to human Rad51. This work is supported by in part by Grants-in-Aid from the Ministry of Education, Science and Culture of Japan.

References

1 Shiloh, Y. and Kastan, M. B. (2001) ATM: genome stability, neuronal development, and cancer cross paths. *Adv. Cancer Res.* **83,** 209-254

2 Goff, S. P., Gilboa, E., Witte, O. N. and Baltimore, D. (1980) Structure of the Abelson murine leukemia virus genome and the homologous cellular gene: studies with cloned viral DNA. *Cell* **22,** 777-85

3 Baskaran, R., Wood, L. D., Whitaker, L. L., Canman, C. E., Morgan, S. E., Xu, Y., Barlow, C., Baltimore, D., Wynshaw-Boris, A., Kastan, M. B. and Wang, J. Y. (1997) Ataxia telangiectasia mutant protein activates c-Abl tyrosine kinase in response to ionizing radiation. *Nature* **387,** 516-519

4 Shafman, T., Khanna, K. K., Kedar, P., Spring, K., Kozlov, S., Yen, T., Hobson, K., Gatei, M., Zhang, N., Watters, D., Egerton, M., Shiloh, Y., Kharbanda, S., Kufe, D. and Lavin, M. F. (1997) Interaction between ATM protein and c-Abl in response to DNA damage. *Nature* **387,** 520-523

5 Sawyers, C. L., McLauphlin, J., Goga, A., Havlik, M. and Witte, O. N. (1994) The nuclear tyrosine kinase c-Abl negatively regulates cell growth. *Cell* **77,** 121-131

6 Yuan, Z. M., Huang, Y., Whang, Y., Sawyers, C., Weichselbaum, R., Kharbanda, S. and Kufe, D. (1996) Role for c-Abl tyrosine kinase in growth arrest response to DNA damage. *Nature* **382,** 272-274

7 Yuan, Z. M., Huang, Y., Ishiko, T., Kharbanda, S., Weichselbaum, R. and Kufe, D. (1997) Regulation of DNA damage-induced apoptosis by the c-Abl tyrosine kinase. *Proc Natl Acad Sci U S A* **94,** 1437-1440

8 Agami, R., Blandino, G., Oren, M. and Shaul, Y. (1999) Interaction of c-Abl and p73a and

their collaboration to induce apoptosis. *Nature* **399,** 809-813

9 Gong, J., Costanzo, A., Yang, H.-Q., Melino, G., Kaelin, W. G. J., Levrero, M. and Wang, J. Y. J. (1999) The tyrosine kinase c-Abl regulates p73 in apoptic response to cisplatin-induced DNA damage. *Nature* **399,** 806-809

10 Yuan, Z., Shioya, H., Ishiko, T., Sun, X., Gu, J., Huang, Y., Lu, H., Kharbanda, S., Weichsekbaum, R. and Kufe, D. (1999) p73 is regulated by tyrosine kinase c-Abl in the apoptotic response to DNA damage. *Nature* **399,** 814-817

11 Yuan, Z.-M., Huang, Y., Ishiko, T., Nakada, S., Utsugisawa, T., Kharbanda, S., Wang, R., Sung, P., Shinohara, A., Weichselbaum, R. and Kufe, D. (1998) Regulation of Rad51 function by c-Abl in response to DNA damage. *J. biol. Chem.* **273,** 3799-3802

12 Chen, G., Yuan, S. S., Liu, W., Xu, Y., Trujillo, K., Song, B., Cong, F., Goff, S. P., Wu, Y., Arlinghaus, R., Baltimore, D., Gasser, P. J., Park, M. S., Sung, P. and Lee, E. Y. (1999) Radiation-induced assembly of Rad51 and Rad52 recombination complex requires ATM and c-Abl. *J Biol Chem* **274,** 12748-12752

13 Shinohara, A. and Ogawa, T. (1995) Homologous recombination and the roles of double-strand breaks. *Trends Biochem. Sci.* **20,** 387-391

14 Sonoda, E., Sasaki, M. S., Buerstedde, J.-M., Bezzubova, O., Shinohara, A., Ogawa, H., Takata, M., Yamaguchi-Iwai, Y. and Takeda, S. (1998) Rad51-deficient vertebrate cells accumulate chromosomal breaks prior to cell death. *EMBO J.* **17,** 598-608

15 Kruh, G. D., Perego, R., Miki, T. and Aaronson, S. A. (1990) The complete coding sequence of *arg* defines the Abelson subfamily of cytoplasmic tyrosine kinases. *Proc. Natl. Acad. Sci. USA* **87,** 5802-5806

16 Cazzaniga, G., Tosi, S., Aloisi, A., Giudici, G., Daniotti, M., Pioltelli, P., Kearney, L. and Biondi, A. (1999) The tyrosine kinase Abl-related gene ARG is fused to ETV6 in an AML-M4Eo patient with a t(1;12)(q25;p13): molecular cloning of both reciprocal transcripts. *Blood* **94,** 4370-4373

17 Iijima, Y., Ito, T., Oikawa, T., Eguchi, M., Eguchi-Ishimae, M., Kamada, N., Kishi, K., Asano, S., Sakai, Y. and Sato, Y. (2000) A new ETV6/TEL partner gene, ARG (ABL-related gene or ABL2), identified in an AML-M3 cell line with a t(1;12)(q25;p13) translocation. *Blood* **95,** 2126-2131

18 Shinohara, A., Ogawa, H., Matsuda, Y., Ushio, N., Ikeo, K. and Ogawa, T. (1993) Cloning of human, mouse and fission yeast recombinant genes homologous to Rad51 and RecA. *Nat. Genet.* **4,** 239-243

19 Takao, N., Mori, R., Kato, H., Shinohara, A. and Yamamoto, K. (2000) c-Abl tyrosine kinase is not essential for ataxia telangiectasia mutated functions in chromosomal maintenance. *J. Biol. Chem.* **275,** 725-728

20 Morrison, C., Sonoda, E., Takao, N., Shinohara, A., Yamamoto, K. and Takeda, S. (2000) The controlling role of ATM in recombinational repair of DNA damage. *EMBO J.* **19,** 463-471

21 Takao, N., Kato, H., Mori, R., Morrison, C., Sonoda, E., Sun, X., Shimizu, H., Yoshioka, K., Takeda, S. and Yamamoto, K. (1999) Disruption of ATM in p53-null cells causes multiple functional abnormalities in cellular response to ionizing radiation. *Oncogene* **18,** 7002-7009

22 Slupianek, A., Schmutte, C., Tombline, G., Nieborowska-Skorska, M., Hoser, G., Nowicki, M. O., Pierce, A. J., Fishel, R. and Skorski, T. (2001) BCR/ABL regulates mammalian RecA homologs, resulting in drug resistance. *Mol. Cell* **8,** 795-806

23 Liu, Z.-G., Baskaran, R., Lea-Chou, E. T., Wood, L. D., Chen, Y., Karin, M. and Wang, J. Y. J. (1996) Three distinct signalling responses by murine fibroblasts to genotoxic stress. *Nature* **384,** 273-276

24 Haaf, T., Golub, E. I., Reddy, G., Radding, C. M. and Ward, D. C. (1995) Nuclear foci of mammalian Rad51 recombination protein in somatic cells after DNA damage and its localization in synaptonemal complexes. *Proc. Natl. Acad. Sci. U.S.A.* **92,** 2298-2302

25 Koleske, A. J., Gifford, A. M., Scott, M. L., Nee, M., Bronson, R. T., Miczek, K. A. and Batimore, D. (1998) Essetial roles for the Abl and Arg tyrosine kinases in neurulation. *Neuron* **21,** 1259-1272

26 Wang, B. and Kruh, G. D. (1996) Subcellular localization of the Arg protein tyrosine kinase. *Oncogene* **13,** 193-197

27 Van Etten, R. A. (1999) Cycling, stressed-out and nervous: cellular functions of c-Abl. *Trends in Cell Biol.* **9,** 179-186

Figure Legends

Figure 1 Targeted disruption of the *Arg* gene.

(A) Schematic representation of part of the chicken *arg* locus and configuration of the targeted loci. Solid boxes indicate the positions of exons encoding the N-terminal portion of the chicken Arg tyrosine kinase domain. (B) Southern blot analysis of the chicken *Arg* locus. KpnI-digested

genomic DNA from wild-type, heterozygous *Arg* mutant (*Arg*$^{+/-}$), and homozygous *Arg* mutant (*Arg*$^{-/-}$) DT40 cells was hybridized with the probe shown in panel (A). (C) RT-PCR analysis of Arg mRNA expression in wild-type and homozygous *Arg* mutant (*Arg*$^{-/-}$) DT40 cells.

Figure 2 IR-induced Rad 51 focus formation in *Arg*-deficient cells.

(A) Immunofluorescence visualization of Rad51 foci in cells of the genotypes indicated, before and 3 hours after 4 Gy X-ray irradiation. (B) Quantitation of Rad51 focus formation in the wild-type and mutant DT40 cells following irradiation. The cumulative numbers of Rad51 foci are presented per 100 cells and show representative results from three separate experiments.

Figure 3 IR- induced chromosomal aberrations in *Arg*-deficient cells.

Cells were subjected to 2 Gy X-ray irradiation, then incubated with colcemid for 3 hours, and harvested. The cumulative numbers of chromosomal aberrations are presented as macrochromosomal (1-5 and Z) gaps and breaks per 100 metaphase spreads. Each value represents the mean $\pm$ S.D. (n = 3).

Figure 4 Arg associates with and phosphorylates Rad51 in vivo

293T cells were cotransfected with 0.5 mg of Flag-tagged expression vectors encoding wild-type (wt, lane 1) or kinase-dead (kd, lane 2) Arg and 0.5 mg of the HA-tagged Rad51 expression vector; as controls, wt (lane 3) or kd (lane 4) c-Abl expression vectors were also cotransfected with HA-tagged Rad51 expression vectors. Forty-eight hours after transfection, cellular lysates were immunoprecipitated (IP) with anti-Flag (first row) or anti-HA (second row) antibodies, and the immunoprecipitates were subjected to immunoblot (IB) analysis using anti-HA (first row) or anti-phosphotyrosine (P-Tyr) (second row) antibodies. To check the protein expression levels, 4% of the cellular lysates were directly subjected to immunoblot analysis using either anti-Flag (third

row) or anti-HA (fourth row) antibodies.

Table 1　Radiosensitivity of wild-type and mutant DT40 cells as assessed by clonogenic survival following X-ray irradiation

Genotype	control	Survival（%）	
		4Gy	8Gy
Wild type	100	10.4 ± 0.35	0.82 ± 0.08
ATM $^{-/-}$	100	2.2 ± 0.11	0.027 ± 0.001
c-Abl $^{-/-}$	100	12.0 ± 0.61	0.65 ± 0.07
Arg $^{-/-}$	100	6.9 ± 0.59	0.37 ± 0.04

Each value represents the mean ± S.D. (n = 3) for at least three separate experiments.

Table 2 Targeted integration frequencies in *Arg*-deficient DT40 cells

		Targeted integration frequencies	
Locus	selection drug	wild type	*Arg*$^{-/-}$
ATM	blasticidin-S	61%（22／36）	24%（9／38）
JSAP2	blasticidin-S	95%（41／43）	70%（30／43）
ATR	puromycin	68%（21／31）	43%（9／21）

Values shown are percentage of clones containing targeting constructs relative to the total number of drug-resistant clones analyzed (absolute numbers are given in parentheses).

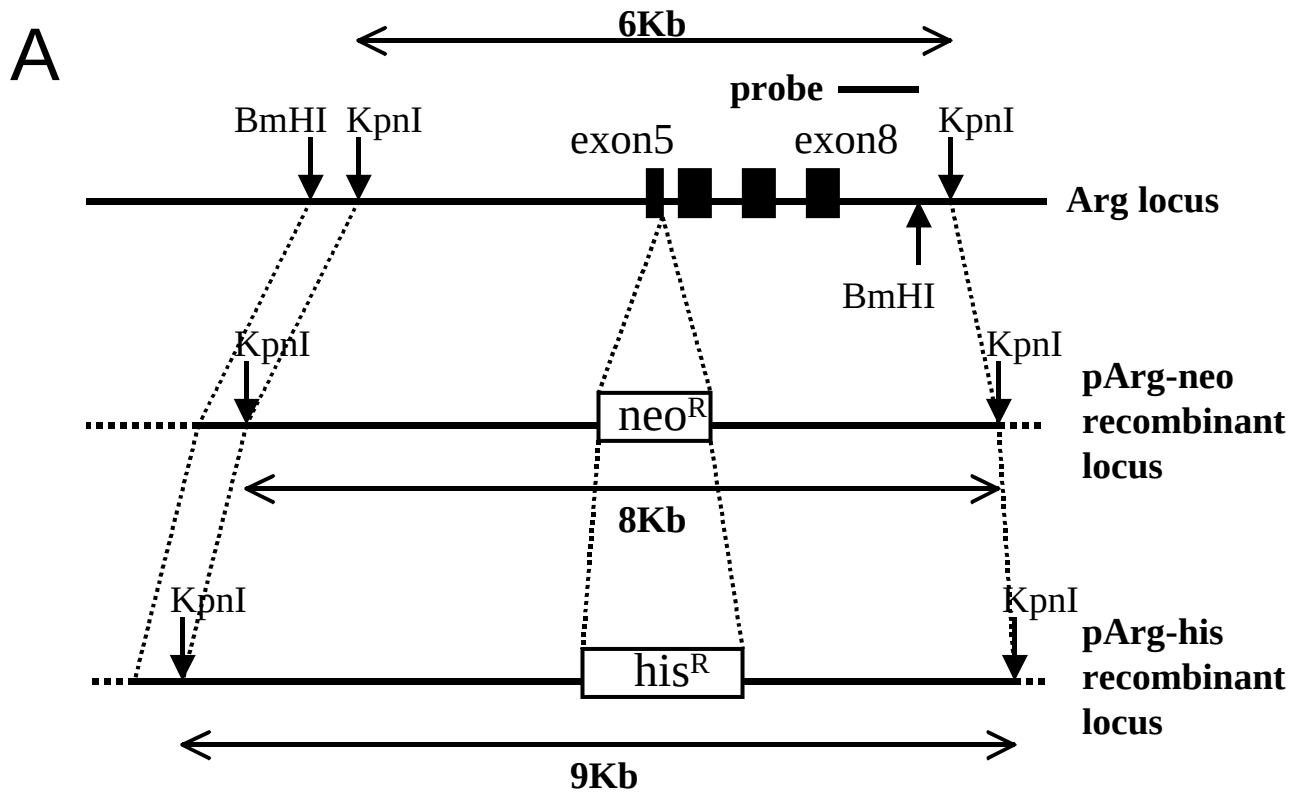
A
6Kb
probe
BmHI
KpnI
exon5
exon8
KpnI
Arg locus
BmHI
KpnI
KpnI
neo^R
pArg-neo recombinant locus
8Kb
KpnI
KpnI
his^R
pArg-his recombinant locus
9Kb

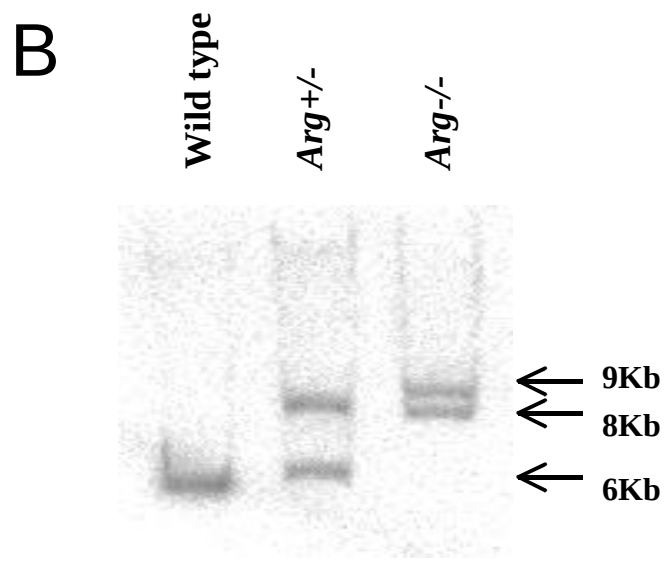
B
Wild type
Arg+/-
Arg-/-
9Kb
8Kb
6Kb

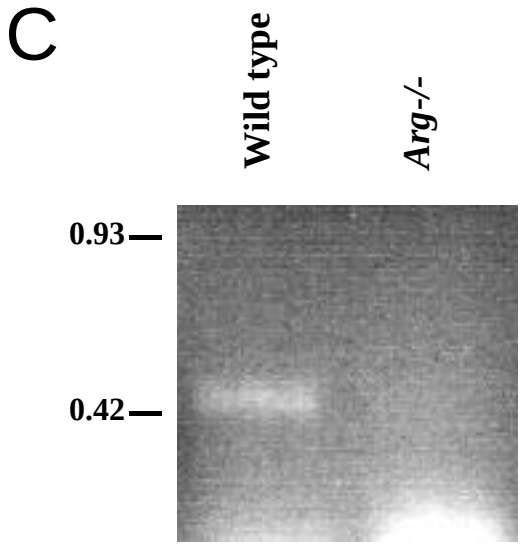
C
Wild type
Arg-/-
0.93
0.42

Fig 1, Li et al

A

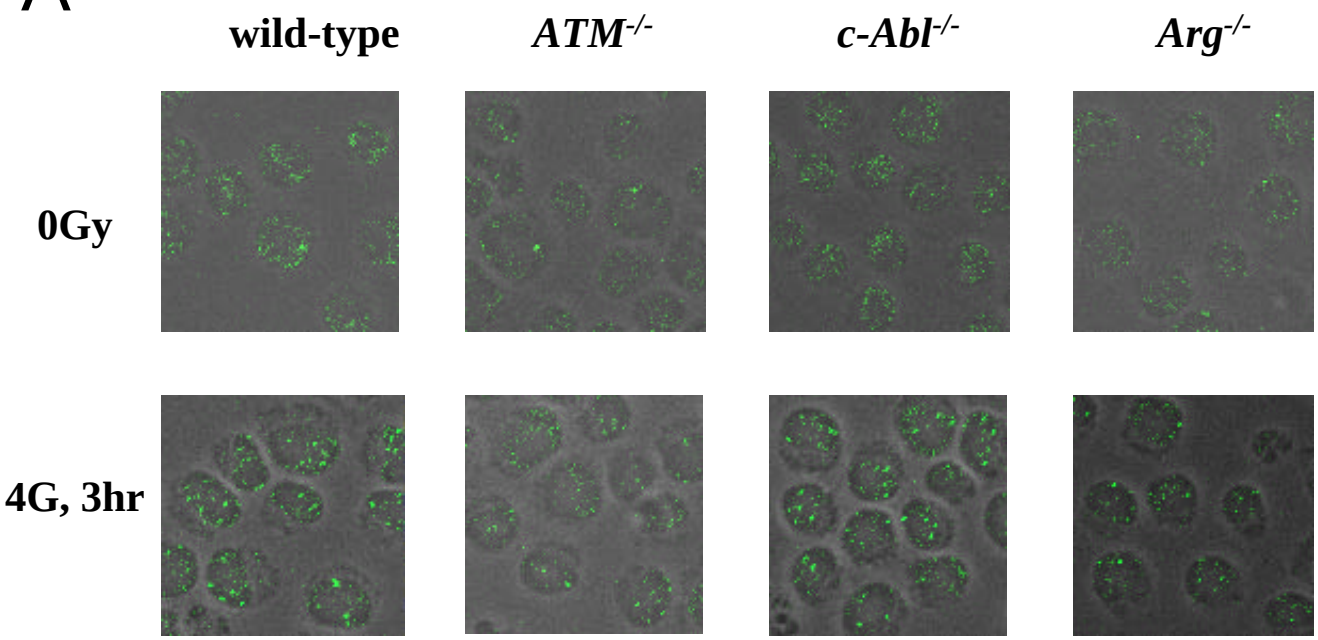

B

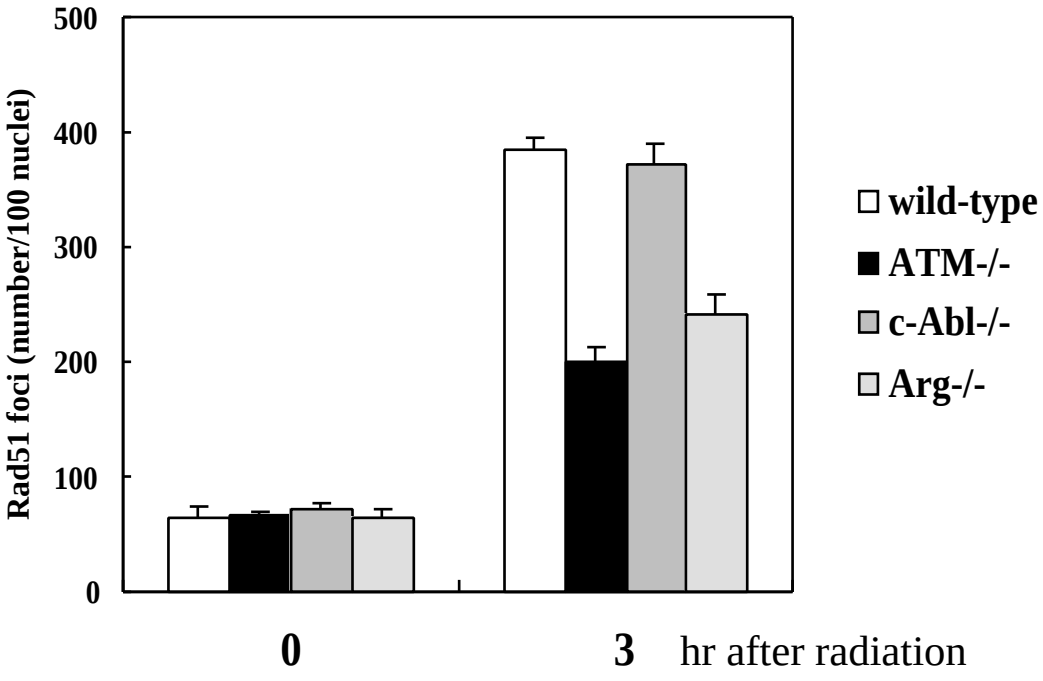

Fig 2, Li et al

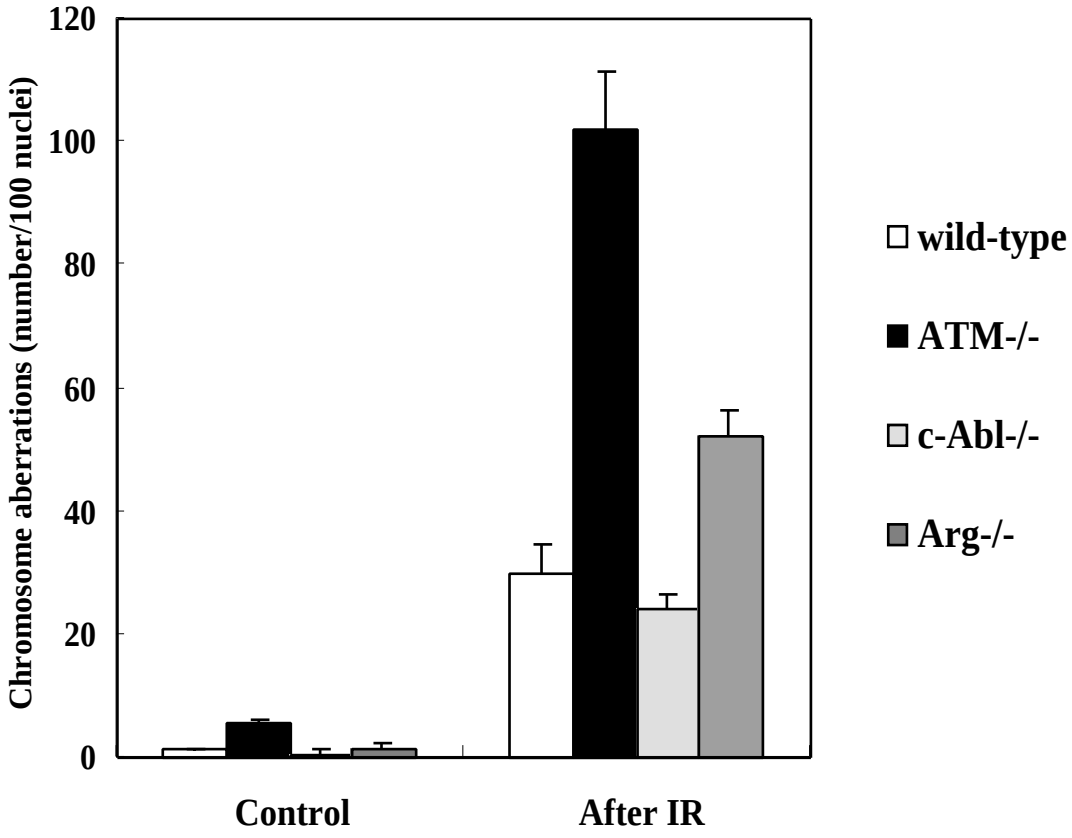
120
100
80
60
40
20
0
Chromosome aberrations (number/100 nuclei)
Control
After IR
wild-type
ATM-/-
c-Abl-/-
Arg-/-

Fig 3, Li et al

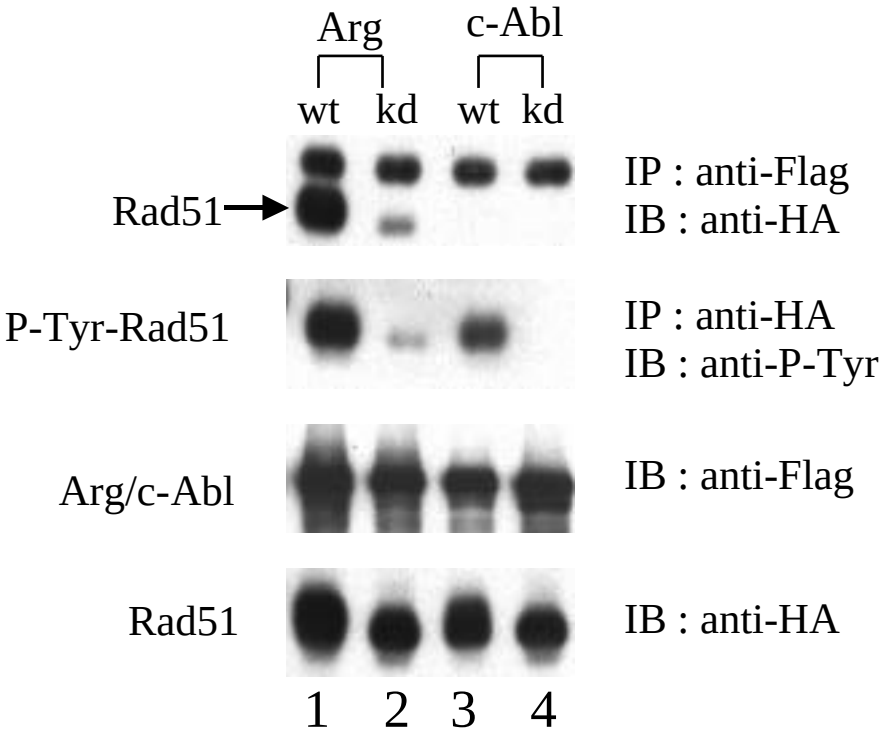
Arg
c-Abl
wt
kd
wt
kd
Rad51
IP : anti-Flag
IB : anti-HA
P-Tyr-Rad51
IP : anti-HA
IB : anti-P-Tyr
Arg/c-Abl
IB : anti-Flag
Rad51
IB : anti-HA
1
2
3
4

Fig 4, Li et al